These equalities correspond to the velocities of some of the long elastic waves being zero. At low frequencies, $G(\omega)$ then becomes similar to the frequency spectrum of a one- or two-dimensional lattice. In practice, the elastic constants of any real crystal do not satisfy any of these equalities, though in some cases they are nearly satisfied.

Finally, we write down the expression for Θ_T for Ag obtained by using in (20) the values of the elastic constants given in (11):

$$\Theta_T=\Theta_0\left[1-\frac{22}{3}\left(\frac{T}{\Theta_0}\right)^2\right],$$

$$T\ll\Theta_0 \quad \text{and} \quad \Theta_0\sim 225°\text{K}. \quad (25)$$

From (25) one sees that the theoretical $\Theta-T$ curve for Ag is very flat near 0°K; for example, $\Theta_0-\Theta_5\sim 0.8°\text{K}$.

Low-Temperature Behavior of the Θ-T Curve for Body-Centered Cubic Metals

We have made an analysis similar to that given above from the solutions of the secular equation given in I for body-centered cubic metals. In this case α_2/α_1 of (20) is always positive, provided the elastic constants satisfy the conditions (21a) and (21b). Thus, for b.c.c. metals, the $\Theta-T$ curve calculated on the basis of the secular equation given in I will not have a maximum at a low nonzero temperature.[20] It should be mentioned that the experimental $\Theta-T$ curve for sodium does exhibit a maximum at about 2 or 3°K.

The formula governing the fall of Θ for sodium as the temperature is increased above zero is

$$\Theta_T=\Theta_0\left[-\frac{210}{3}\left(\frac{T}{\Theta_0}\right)^2\right],$$

$$T\ll\Theta_0 \quad \text{and} \quad \Theta_0\sim 139°\text{K}. \quad (26)$$

The theoretical rate of fall of Θ with increasing T is much greater here than for Ag.

[20] It may be mentioned that if $\epsilon>0$, the $\Theta-T$ curve for both b.c.c. and f.c.c. metals can have a maximum at a low nonzero temperature for suitable values of the elastic constants.

PHYSICAL REVIEW VOLUME 98, NUMBER 6 JUNE 15, 1955

Multiple Scattering of Slow Neutrons by Flat Specimens and Magnetic Scattering by Zinc Ferrite*

B. N. BROCKHOUSE,† *Physics Division, Atomic Energy of Canada Limited, Chalk River, Ontario, Canada*

AND

L. M. CORLISS AND J. M. HASTINGS, *Chemistry Department, Brookhaven National Laboratory, Upton, New York*

(Received March 7, 1955)

Measurements of scattering from Be, Pb, Bi, and Th under conditions where multiple scattering predominated were compared with predictions based on the work of Chandrasekhar and of Vineyard. Good agreement was obtained. A table of values of the expected multiple scattering by flat specimens is given. These results were used to correct measurements of diffuse scattering by zinc ferrite at room temperature and higher to obtain the differential magnetic cross section of the magnetic ions. The cross section shows interesting features which are discussed. At liquid nitrogen temperatures a small-angle scattering effect was found. This is interpreted as arising from short-range ferromagnetic ordering of the iron ions.

INTRODUCTION

MEASUREMENTS of the angular distribution of neutrons which are diffusely scattered by a paramagnetic substance can, in principle, lead to a determination of the spatial distribution of the magnetic electrons[1,2] and to information on the interactions between the magnetic ions.[3,4] It is necessary to obtain the angular distribution rather accurately, if more than the most qualitative information is to be gained. In particular it is necessary to have accurate information at small scattering angles if a questionable appeal to theory in extrapolating the scattering curve to zero scattering angle is to be avoided.[3] The apparatus used in these experiments was designed to permit working as close to the main beam as the angular acceptance of the counters would permit, under conditions of low and flat background. The diffusely scattered neutrons have a number of sources in addition to magnetic scattering, the most important being nuclear incoherent scattering, nuclear thermal diffuse coherent scattering and multiple scattering. In this paper a method of subtracting multiple scattering is described and experimentally verified.

* Research carried out at Brookhaven National Laboratory under the auspices of the U. S. Atomic Energy Commission. This paper was presented at the Chicago Meeting of the American Physical Society, November 27–28, 1953.

† Guest scientist in the Reactor Department, Brookhaven National Laboratory from April, 1953, to February, 1954.

[1] O. Halpern and M. H. Johnson, Phys. Rev. **55**, 898 (1939).
[2] Shull, Strauser, and Wollan, Phys. Rev. **83**, 333 (1951).
[3] J. H. Van Vleck, Phys. Rev. **55**, 924 (1939).
[4] P. J. Bendt, Phys. Rev. **89**, 561 (1953).

According to Halpern and Johnson[1] the differential scattering cross section of a free paramagnetic ion in an S state is

$$\sigma_{\text{mag}}=\frac{8\pi}{3}S(S+1)\left(\frac{e^2}{mc^2}\gamma\right)^2 f^2,\ \text{cm}^2/(4\pi\ \text{steradians}), \quad (1)$$

where S is the spin of the ion and γ is the magnetic moment of the neutron in nuclear magnetons. The form factor, f, is defined by

$$f=\int\int\int \psi^2 \exp(i\mathbf{q}\cdot\mathbf{r})dV, \quad (2)$$

where $\mathbf{q}$ is the vector change in momentum of the neutron. For a spherically symmetrical distribution (S-state),

$$f=\int_0^\infty r^2|\psi(r)|^2\frac{\sin\mu r}{\mu r}dr\equiv\int_0^\infty N(r)\frac{\sin\mu r}{\mu r}dr, \quad (3)$$

where $\mu=4\pi\sin\theta/\lambda$, ψ is the wave function of the appropriate spin shell normalized to make $f=1$ for $\mu=0$ and $N(r)$ is the spin distribution.

If the ions are coupled together so that the neutron can be scattered inelastically, the form factor in the forward direction is reduced from the value unity which applies to elastic scattering.[3] If in addition short-range ordering of the spins occurs the measured differential cross section per ion can be strongly altered from that given by Eq. (1), the form of the cross section being dependent on the details of the ordering. These effects have been observed by Bendt[4] and by Shull, Strauser, and Wollan.[2]

The dependence of the cross section on the spin distribution $N(r)$ is contained in the form factor, which can, in principle, be inverted to obtain the distribution. For such an inversion to give details of the distribution the measurements must extend over the entire range of μ in which f is appreciably different from zero. Because f is proportional to the square root of the cross section and therefore the intensity, this is a difficult condition to fulfill. The difficulty is aggravated by the fact that at large angles where the magnetic scattering is small, the thermal diffuse scattering is large and no satisfactorily accurate method of calculating it is known. In the present work the authors have tried to obtain accurate values of f, but the results do not justify inversion and a simpler method of analysis is used.

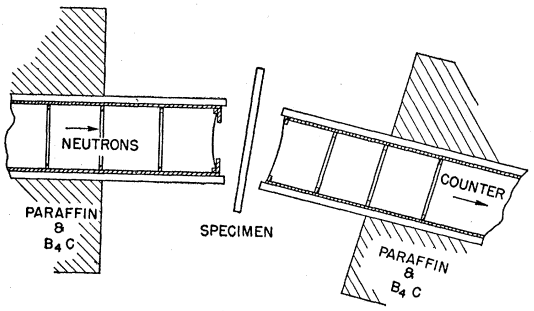

FIG. 1. Experimental arrangement.

EXPERIMENTAL ARRANGEMENTS AND METHODS

Two evacuated cadmium-lined collimators (Fig. 1) were added to the crystal spectrometer previously described[5] which was set for a wavelength of 1.062 A. The specimen in the form of a flat slab was mounted on the spectrometer table which was rotated at one half the speed of the counter. When temperatures other than room temperature were required the specimen was supported inside an evacuated scattering chamber which formed part of a liquid-nitrogen cryostat and which could also be used as a furnace.

To minimize air scattering, the air spaces between the evacuated collimators were kept as small as possible. Cadmium apertures intercepted neutrons scattered by the cadmium lining of the collimators, hence only those neutrons which were scattered twice by cadmium contributed to the background. Since the probability of a single scattering is about[6] 0.002 at our wavelength, the contribution from the double process is negligible.

A typical scattering pattern is shown in Fig. 2. The background with no specimen is also shown. To obtain the background with specimen, cadmium differences were measured. The net counting rate, N, is taken as

$$N=(N-N_{cd})_s-T(N-N_{cd})_b, \quad (4)$$

where T is the transmission of the specimen. The subscript cd refers to measurements made with 0.025 inch of cadmium in the beam, the subscripts s and b refer to measurements with and without specimen respectively.

Cross sections were computed as follows. The counting rate from diffuse elastic scattering may be expressed as

$$N=\left\{P_0\epsilon\frac{A}{4\pi r^2}\right\}S(2\theta)\equiv\left\{P_0\epsilon\frac{A}{4\pi r^2}\right\}S_0\sec\theta(T)^{\sec\theta-1}, \quad (5)$$

where $S(2\theta)d\Omega/4\pi$ is the fraction of the incident beam scattered into a solid angle $d\Omega$ and where P_0 is the number of neutrons in the beam per unit time, ϵ is the counter efficiency, A is the area of the collimator end, and r is its distance from the specimen.

The diffuse scattering cross section/(4π steradians)/molecule is

$$\sigma=\frac{1}{nT}(S_0-S_{M0})=\frac{1}{n(T)^{\sec\theta}\sec\theta}[S(2\theta)-S_M(2\theta)], \quad (6)$$

[5] Corliss, Hastings, and Brockman, Phys. Rev. **90**, 1013 (1953).
[6] B. N. Brockhouse, Can. J. Phys. **31**, 432 (1953).

where n is the number of molecules/cm^2 in the specimen and S_M represents the fraction multiply scattered computed as described in the following section. This diffuse scattering cross section is the sum of the nuclear incoherent, the magnetic diffuse and the coherent thermal diffuse cross sections, plus any diffuse scattering from defects. The cross sections were put on an absolute basis by comparison with the coherent scattering peaks of a nickel powder specimen. A value, $\sigma_{\text{coh}}=13.2\pm0.2$ barns for the coherent cross section of nickel as given by the U.S.A.E.C. Cross-Section Committee[7] and a value $2B=0.766\times10^{-16}$ for the constant in the Debye-Waller factor for nickel at room temperature were assumed. The integrated intensity of a peak is given by the usual formula

$$I_{hkl}=\left\{P_0\epsilon\frac{A}{4\pi r^2}\right\}\frac{\lambda^3}{\omega}\left[\frac{wN_A}{zMv}\right](T)^{\sec\theta}\times\exp\left[-2B\left(\frac{\sin\theta}{\lambda}\right)^2\right]\frac{(jF^2)_{hkl}}{\sin^2 2\theta}, \quad (7)$$

where ω is the angular velocity of the counter, w is the weight per unit area of the specimen, z is the number of molecules per unit cell, M is the molecular weight, v is the volume of a unit cell, N_A is Avogadro's number, θ is the Bragg angle, j is the multiplicity of the plane hkl, and F^2 is the structure factor for the plane.

To check the calibration the cross section of vanadium metal was measured near the forward direction, with the result that $\sigma_{\text{incoh}}=5.14$ barns/4π steradians as compared with the value 5.1 ± 0.1 barns accepted by the cross-section committee.[7]

Powdered specimens were contained in cassettes having $\frac{1}{32}$-inch aluminum windows. As the incoherent cross sectio of aluminum was measured and found to be less than 0.08 barn, no correction for incoherent scattering by the cassettes was necessary.

To correct for thermal diffuse scattering, the well-known "independent vibrations" approximation was used, purely for want of a better practical method. Thus we have taken

$$\sigma_{\text{T.D.}}=\sigma_{\text{coh}}[1-\exp[-2B(\sin\theta/\lambda)^2]]. \quad (8)$$

Where necessary, small corrections were applied for contamination of the beam by second-order neutrons, for effects of thermal expansion, and for thermal diffuse scattering by the aluminum windows of the cassettes.

MULTIPLE SCATTERING

The problem of multiple scattering in flat specimens was studied in some detail with a view to finding a satisfactory prescription for correction of magnetic and other diffuse scattering measurements. Following a suggestion by Vineyard,[8] multiple scattering calculations of Chandrasekhar[9] were reduced to a form suitable for easy application. Since the calculations apply to ideal experimental conditions not often met in practice, approximate corrections for deviation from the ideal geometry were computed. Measurements on a series of specimens in which multiple scattering is the major source of diffuse scattering showed that the method of treatment is satisfactory.

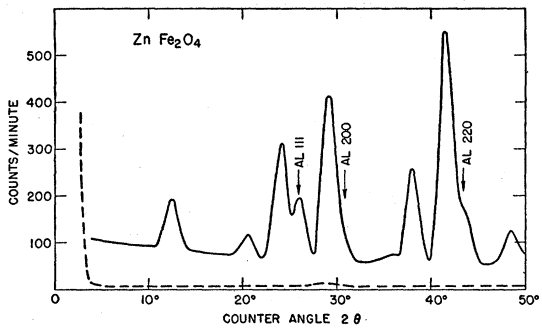

FIG. 2. Scattering pattern of $ZnFe_2O_4$ (solid line) and background with no specimen (dashed line). The transmission of the zinc ferrite specimen was 0.85.

In Chandrasekhar's treatment two parameters occur: the macroscopic total cross section of the specimen $\tau=\log_e T$, and the quantity $\omega=1-n\sigma_a/\tau$, where σ_a is the capture cross section per molecule and n is the number of molecules/cm^2. For isotropic primary scattering, the multiple scattering is a function of these two variables alone. The total scattering (at various angles) of neutrons incident normally on the flat specimen, was computed from Eq. (16), page 211 of reference 9, modified for use with neutrons. The multiple scattering was found by subtracting the primary scattering

$$\omega(e^{-\tau}-e^{-\tau\sec\theta})/(\sec\theta-1),$$

and then extrapolated graphically to the forward direction. This procedure was necessary because the expression for the multiple scattering is indeterminate when the angle of scattering equals the angle of incidence. The results are shown in columns 2 to 6 of Table I for values of ω from 0.5 to 1.0 (The tables of the functions[9] used in the computations only extend over this range of values.) The multiple scattering for smaller values of ω was calculated using the values for $\omega=1$, Vineyard's second order calculations[8] for $\omega=1$, the theorem that the multiple scattering can be expanded as a power series in ω corresponding to the different orders of scattering,[8,10] and the plausible assumption that the ratio of successive orders higher than the first

[7] *Neutron Cross Sections*, Atomic Energy Commission Report AECU-2040 and supplements (Technical Information Division, Department of Commerce, Washington, D. C., 1952).

[8] G. H. Vineyard, Phys. Rev. **96**, 93 (1954), and private communication. We are indebted to Dr. Vineyard for an advance copy of his calculations of second-order scattering.

[9] S. Chandrasekhar, *Radiative Transfer* (Clarendon Press, Oxford, 1950); Chandrasekhar, Elbert, and Franklin, Astrophys. J. **115**, 244 (1952).

[10] J. Tittman and C. Sheer, Phys. Rev. **83**, 746 (1951).

TABLE I. Multiple scattering in the forward direction (S_{M0}), computed following Chandrasekhar and Vineyard as discussed in the text.

$\tau \backslash \omega$	1.0	0.95	0.9	0.8	0.5	0.3	0.2	0.1	0.05
0.05	0.00515	0.00467	0.00421	0.00325	0.00127	0.000432	0.000190	0.000047	0.0000117
0.10	0.0177	0.0157	0.0139	0.0108	0.00402	0.00139	0.000605	0.000148	0.0000368
0.15	0.0356	0.0313	0.0289	0.0214	0.00780	0.00269	0.00117	0.000286	0.0000707
0.20	0.0578	0.0513	0.0452	0.0343	0.01215	0.00416	0.00180	0.00044	0.000108
0.25	0.0828	0.0731	0.0640	0.0490	0.0171	0.00570	0.00245	0.000594	0.000146
0.50	0.2435	0.210	0.1795	0.134	0.0432	0.0142	0.00597	0.00142	0.000348

is a constant. Good agreement was obtained between the two methods of calculation in their range of overlap.

Spot calculations showed that the angular dependence of the multiple scattering was closely the same as the primary scattering, *viz.*,

$$S_M(2\theta) = S_{M0} \sec\theta \exp[-\tau(\sec\theta - 1)],$$

at least up to $\tau = 0.25$ and scattering angle of 90°. The calculations are based on the assumption that primary scattering is isotropic. For all except the lightest elements this is a good approximation for incoherent scattering. Coherent scattering is concentrated in Debye-Scherrer cones, and hence is far from isotropic unless angular regions much larger than line separations are considered.

In order to determine whether this method of treating multiple scattering can justly be applied to coherent scattering by polycrystalline materials, measurements were made on a series of specimens of lead, bismuth, beryllium, and thorium. Near the forward direction, multiple scattering is the major source of diffuse scattering in these materials.[11] For thorium $\omega = 0.75$, for the others $\omega = 1.0$.[7] Some of the scatterers were sheet material with considerable preferred orientation. Figure 3 shows the measured diffuse scattering by these specimens in an angular range of about 10° near the forward direction, and the computed multiple scattering for $\omega = 1.0$ and $\omega = 0.75$. The experimental points must be corrected for thermal diffuse scattering according to Eq. (8). Also, because the theoretical curves were calculated for an extended source, scatterer, and counter, they do not apply precisely to the geometry of this experiment. Rather than modify the theoretical curves, we have chosen to apply a correction to the experimental points. Referring to the insert in Fig. 3, it can be seen that the source of multiply-scattered neutrons is more extended than the source of singly-scattered neutrons. In the experimental arrangement (Fig. 1) some of the neutrons multiply-scattered in the desired direction would not have been counted because they were excluded by the collimation. Calibration is carried out, however, by comparison with singly-scattered neutrons. Hence the measured multiple scattering is lower than the multiple scattering calculated for an extended scatterer and detector.

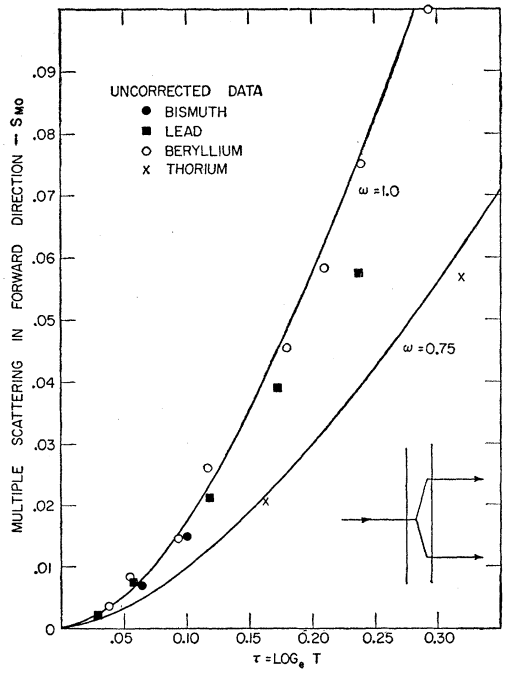

FIG. 3. The measured diffuse scattering near the forward direction plotted as a function of the parameter τ for various scatterers. The solid curves are calculated multiple scattering curves.

The fraction of *doubly*-scattered neutrons (η) which miss the counter because of this effect has been computed, using the isotropic approximation for the primary scattering, by calculating the fraction of doubly scattered neutrons which underwent their second scattering at a position in the specimen outside the area "seen" by the counter collimator. The integrals were evaluated numerically. In general η is a function of two parameters in addition to τ, *viz.*,

t = specimen thickness/counter collimator diameter,

ξ_0 = beam diameter/counter collimator diameter.

A sufficient condition that the correction be negligible is that $\tau(1-\xi_0)/t \gg 1$. The correction is fairly small if $\tau/t > 1$ and $\xi_0 < 1$. Keeping $\xi_0 < 1$ has the additional advantage that accidental variations in the angular sensitivity for single scattering are minimized. A further approximation was made in the computations. All

[11] Thorium is monoisotopic and has zero spin and therefore gives no incoherent scattering. The others have been shown to have very small incoherent cross sections by experiment (see reference 7).

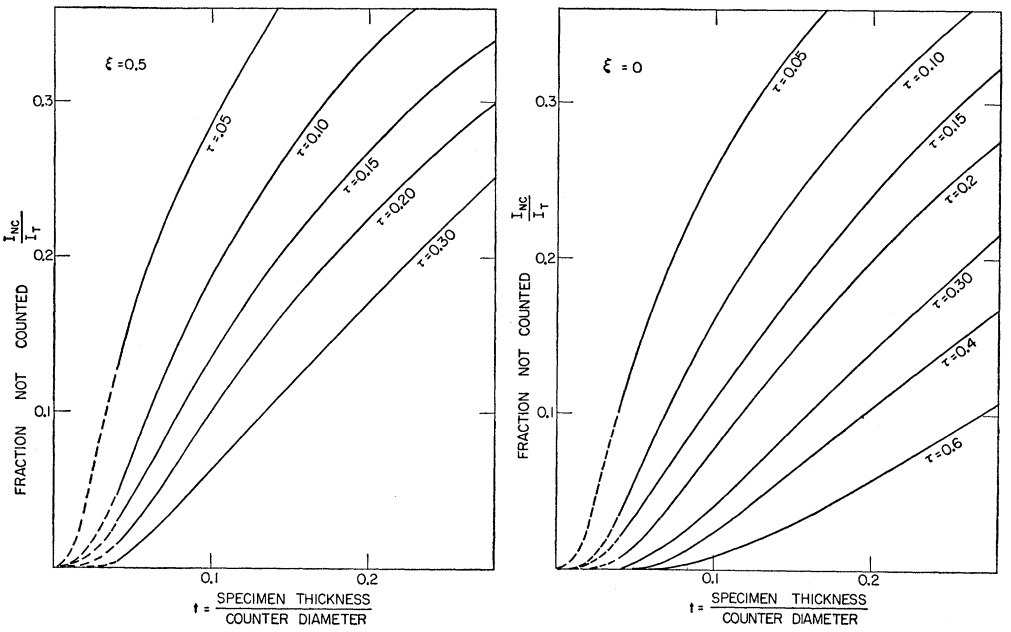

FIG. 4. Fraction of doubly scattered neutrons not counted for various thicknesses of scatterer. (a) Parameter $\xi=0.5$ based on $\xi_0=0.7$ as in this experiment. (b) $\xi=\xi_0=0$, pencil beam.

neutrons were assumed incident at a radial distance ξ from the center of the beam (in units of the counter diameter). For the apparatus $\xi_0=0.7$ and the computations were made for the case $\xi=(0.707\xi_0)=0.5$, corresponding to the mean radius of the beam. Computations were also made for the case of a pencil beam, $\xi=\xi_0=0$. The results are shown in Figs. 4(a) and 4(b).

The computed corrections ranged from a few percent for the beryllium specimens up to 35 percent for the thickest bismuth specimens and were applied to the experimental points of Fig. 3. The results, together with the computed multiple scattering curves for $\omega=0.75$ and 1.0 are shown in Fig. 5. The good agreement is evidence that the isotropic approximation is satisfactory, and gives confidence that this method of treatment of multiple scattering can be generally applied.

MAGNETIC SCATTERING BY ZINC FERRITE

Zinc ferrite[12] was selected as a material for study because the magnetic Fe^{3+} ions are supposedly in S states and therefore the theory of Halpern and Johnson[1] should apply except for possible effects of coupling. These coupling effects would themselves be interesting as an aid to understanding the magnetic properties of the important ferrite group.

The scattering curve at room temperature (Fig. 2) was analyzed near the forward direction and between the Bragg peaks. The results are shown in Fig. 6 as a differential cross section per molecule. In computing the multiple scattering correction, ω was taken to be 0.925.

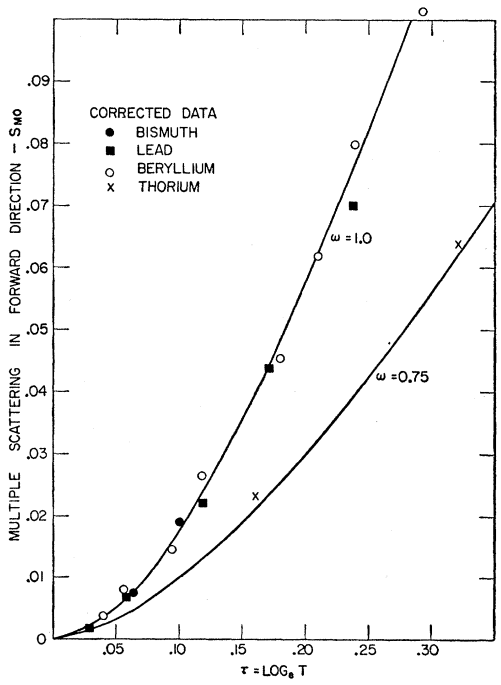

FIG. 5. Diffuse scattering near forward direction as given in Fig. 3 but corrected for thermal diffuse scattering and for neutrons which miss the counter. The solid curves are the same calculated multiple scattering curves as shown in Fig. 3.

[12] The specimen was kindly supplied by Dr. V. C. Wilson of the General Electric Research Laboratories. An analysis by Dr. R. W. Stoenner of Brookhaven National Laboratory showed 45.98 percent iron and 28.33 percent zinc compared with the stoichiometric composition 46.33 percent iron and 27.12 percent zinc.

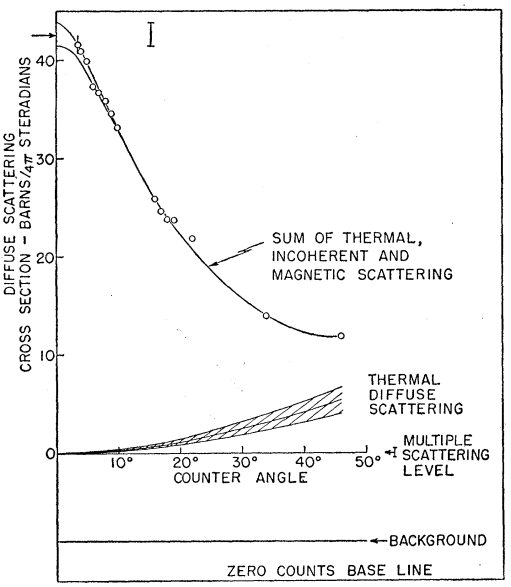

FIG. 6. Measured diffuse scattering cross section of zinc ferrite. The background shown is schematic.

The values of τ for the various specimens were about 0.15 and $t=0.12$, resulting in a value $\eta=0.16$ for the fraction of the multiple scattering that was not counted because of the finite size of counter aperture.

The Debye-Waller constant was found to be $2B=0.99\times10^{-16}$ from a powder pattern taken over an extended angular range, in agreement with an estimate of 0.96×10^{-16} made using the specific heat of Fe_3O_4.[13] The thermal diffuse scattering was calculated from Eq. (8) using the value $2B=0.99\times10^{-16}$. The temperature dependence of the diffuse scattering from 90°K to 450°K was studied, and within the uncertainties, was consistent with the calculated values for the total thermal diffuse scattering, though favoring somewhat smaller values. The incoherent scattering cross section of iron was taken as 0.4 barns/atom,[7] and that of zinc as 0.2 barn.[7] The resulting curve for the magnetic scattering cross section/iron atom is shown in Fig. 7.

The extrapolation to zero scattering angle takes account of the probable persistence to room temperature of a small amount of excess scattering at small angles. This will be discussed in the next paragraph. The extrapolation was made easier by the knowledge that, for small enough angles, the curve must be parabolic and concave downwards (if no short-range ordering occurs).

Estimated limits (broken lines) on the extrapolation are shown. For calculation of the form factor this is the major pertinent uncertainty (in addition to the normal errors of each point). For comparison of the cross section in the forward direction with the theoretical value of 21.2 barns (indicated by an arrow in Fig. 7), errors associated with the normalization of the scattering curve must also be considered. These include possible errors in the determination of the number of atoms/cm² in the specimen, the coherent cross section and other parameters of the nickel standard, and the multiple-scattering level. Estimates of the uncertainty produced by these causes are indicated by vertical bars in the figure. The agreement with the theoretical value is well within the uncertainties.

Small-angle scattering at liquid nitrogen temperature was larger than at room temperature as shown in Fig. 8(a). The temperature dependence of the excess scattering was studied by setting the spectrometer at a fixed angle and allowing the cryostat to warm up, meanwhile recording the counting rate. Measurements were also made at and above room temperature, including a careful comparison of the counting rates at room temperature (295°K) and 500°K. The results are shown in Fig. 8(b). From the figure it appears that a small amount (~2 percent) of the excess scattering persists to room temperature but the strong temperature-dependence suggests that it is probably almost completely absent at 500°K.

DISCUSSION

The presence of the small-angle scattering suggests that there may be short-range coupling between spins at the lower temperatures. A theoretical treatment of scattering of neutrons by such a system has not yet been given, but it seems reasonable to assume that the

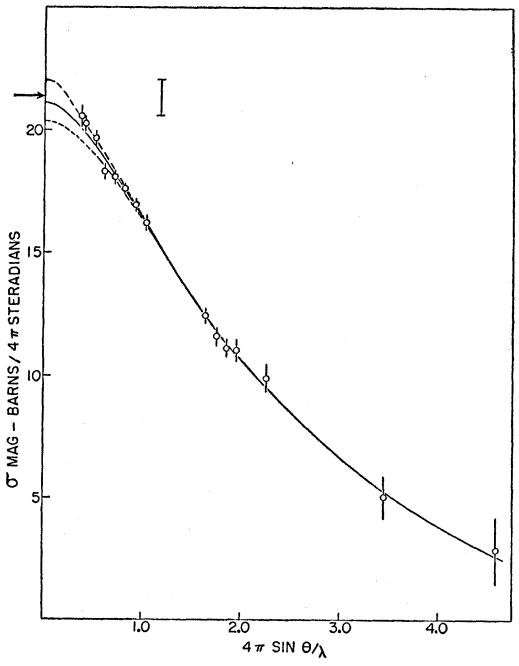

FIG. 7. Magnetic scattering cross section per Fe^{3+} ion in $ZnFe_2O_4$. To the left of the axis of ordinates the arrow indicates the theoretical value 21.2 barns. The short vertical bar opposite the arrow indicates the uncertainty arising from determinate errors as discussed in the text.

[13] R. W. Millar, J. Am. Chem. Soc. **51**, 215 (1929).

result would not be very different from the familiar x-ray result[14]

$$I_M=\sum_{mn} f_m f_n \frac{\sin\mu r_{mn}}{\mu r_{mn}}, \tag{9}$$

where I_M is the measured scattering, f_m and f_n are the scattering factors for atoms m and n, and r_{mn} is the distance between them. For antiferromagnetically coupled atoms, f_m and f_n have opposite signs and, if they are of the same kind, equal magnitudes. For ferromagnetically coupled atoms, f_m and f_n have the same signs. In fact, as shown by the broken line in Fig. 8(a), the experimental results can be fitted by

$$\Delta\sigma=\sigma_{\text{mag}}\,0.31(\sin\mu r/\mu r), \tag{10}$$

with $r=2.98$ A, the shortest distance between iron atoms. This suggests that the effect is caused by ferromagnetic short-range coupling between nearest neighbors, and hence that the interaction between ions on the B (octahedral) sites is ferromagnetic. There is evidence against this interpretation in the properties of mixed ferrites[15] and in the fact, recently established,[16] that zinc ferrite is antiferromagnetic at helium temperatures. This latter fact could be explained by the existence of antiferromagnetic interactions between distant neighbors which are weaker than the ferromagnetic interactions between near neighbors. Such a picture seems reasonable because some distant iron neighbors are coupled by Fe—O—Fe links of large angle, while the nearest neighbors are coupled by 90° links. The importance of large-angle oxygen links in producing antiferromagnetism is now well known.[2,17,18] It should also be pointed out that a small amount of inversion [placing of iron ions on A (tetrahedral) sites] could produce marked effects because of the strong coupling between A and B sites and the large number of B neighbors coupled to any one A site. The degree of inversion of zinc ferrite, established as less than 5 percent,[19] could still be sufficient to produce effects as large as those observed but probably not of the right kind.

Calculations of the magnetic cross section using

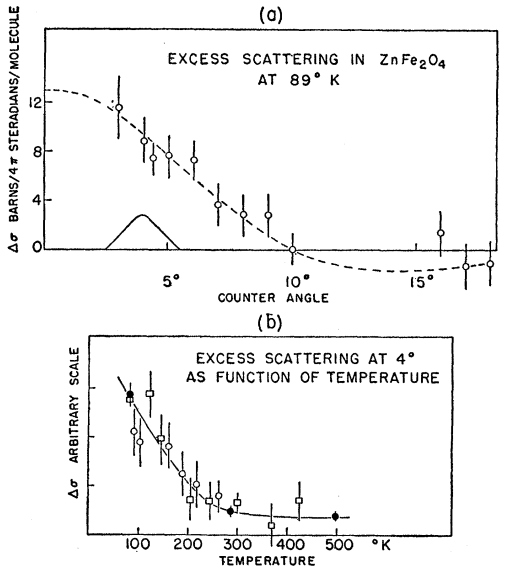

FIG. 8. (a) Difference between the differential scattering cross sections of zinc ferrite at 295°K and 89°K (with a small correction for thermal diffuse scattering applied). The dashed line represents a plot of Eq. (10). (b) Temperature dependence of the scattering at a mean angle of 4 degrees. Different symbols represent the results of different runs.

hydrogenic screened Coulomb wave functions[20] in Eq. (1) were compared with Fig. 7. It was not possible to get a fit within the supposed accuracy of the results. To obtain a fit it was necessary to add a long tail to the spin distribution, the tail comprising about 10 percent of the spins. Such a tail, representing spins not on the iron ions at all but on neighboring ions, might arise simply from persistence to room temperature of the small angle scattering in larger amount than assumed, or it might correspond to the charge transfer or promotion expected to take place in superexchange. The main part of the spin distribution had a maximum at about 0.45 A, in fair agreement with the results for ferromagnetic ferrites,[21] and consistent with the accepted value of 0.67 A for the crystallographic radius of the Fe^{3+} ion.[22]

The authors wish to thank Dr. G. H. Vineyard, Dr. V. C. Wilson, and Dr. R. W. Stoenner for their contributions to the work. One of us (B.N.B.) wishes to express here his deep appreciation of the hospitality he enjoyed at Brookhaven National Laboratory during the time the Chalk River NRX reactor was closed down.

[14] A. H. Compton and S. K. Allison, *X-Rays in Theory and Experiment* (D. Van Nostrand Company, Inc., New York, 1935), second edition, p. 159.
[15] L. R. Maxwell and S. J. Pickart, Phys. Rev. **92**, 1120 (1953).
[16] L. M. Corliss and J. M. Hastings (to be published).
[17] P. W. Anderson, Phys. Rev. **79**, 350; **79**, 705 (1950).
[18] B. N. Brockhouse, Phys. Rev. **94**, 781 (1953).
[19] J. M. Hastings and L. M. Corliss, Revs. Modern Phys. **25**, 114 (1953).
[20] See reference 1, Eq. (7.3).
[21] Corliss, Hastings, and Brockman, Phys. Rev. **90**, 1013 (1953).
[22] R. W. G. Wyckoff, *Crystal Structures* (Interscience Publishers, Inc., New York, 1948), Vol. 1, Chap. III, Table on p. 15.